Journal of Magnetism and Magnetic Materials 361 (2014) 94–98

Contents lists available at ScienceDirect

Journal of Magnetism and Magnetic Materials

journal homepage: www.elsevier.com/locate/jmmm

Spin glass behavior in nanogranular $La_{0.25}Ca_{0.75}MnO_3$ manganites

Antoni Fernández-Martínez [a,b], Antoni García-Santiago [a,b,*], Joan Manel Hernàndez [a,b], Tao Zhang [c]

[a] Grup de Magnetisme, Dept. Física Fonamental, Facultat de Física, Universitat de Barcelona, Martí i Franquès 1, planta 4, edifici nou, 08028 Barcelona, Spain
[b] Institut de Nanociència i Nanotecnologia IN^{2}UB, Universitat de Barcelona, Martí i Franquès 1, planta 3, edifici nou, 08028 Barcelona, Spain
[c] Key Laboratory of Materials Physics, Institute of Solid State Physics, Chinese Academy of Sciences, Hefei 230031, China

ARTICLE INFO

Article history:
Received 8 October 2013
Received in revised form
11 February 2014
Available online 4 March 2014

Keywords:
Manganite
Exchange bias
Charge ordering
Spin-glass behavior
Core–shell model

ABSTRACT

The magnetic properties of two nanogranular $La_{0.25}Ca_{0.75}MnO_3$ manganites with different average grain sizes have been studied. Besides the well-known exchange bias effect and the appearance of ferromagnetic clusters in the grains of both samples, the results show the occurrence of an antiferromagnetic transition and spin-glass properties. Both samples are described as core–shell magnetic systems, whose main difference is found in the interface between the outer ferromagnetic and the inner antiferromagnetic phases of the grains.

1. Introduction

During last several years, perovskite manganites with the general chemical formula $A_{1-x}B_xMnO_3$ (where A is a trivalent rare-earth ion and B is a divalent alkaline earth ion) attracted considerable attention as new magnetic properties emerged as a consequence of a reduction from bulk to nanometric size. When bulk manganites with high values of calcium doping ($x > 0.5$) are cooled below their charge ordering (CO) transition temperature, T_{CO}, an antiferromagnetic (AFM) phase appears where charge carriers localize and orbitals order around the manganese ions [1,2]. This transition is rarely observed when the size of this kind of manganites is reduced to form either nanograins or nanoparticles [3], since this leads to the destruction of the collinear AFM configuration in the surface of these nanometric components [4–6]. In this case, a ferromagnetic (FM)-like spin glass (SG) or cluster glass (CG) behavior is manifested in magnetic measurements [4,7–11]. This behavior is commonly described in the framework of the core–shell model, where FM clusters generally form close to the surface of the nanograins and this allows the occurrence of the exchange bias (EB) interaction with the AFM core [7,9,12,13]. Among other nanosystems, the $La_{0.25}Ca_{0.75}MnO_3$ manganite is a clear example [14] of the effects just described. In this paper, the experimental investigation of the magnetic properties of two nanogranular samples of this composition is reported.

2. Experimental setup

Two nanogranular polycrystalline $La_{0.25}Ca_{0.75}MnO_3$ samples were prepared by the sol–gel method, following the procedure described in [4]. The samples were then annealed at 600 °C (sample *A*) and 1000 °C (sample *B*) during 10 h, getting average grain sizes of 53 nm and 182 nm, respectively, from scanning electron microscope (SEM) images as shown in Fig. 1. Magnetic measurements following zero-field cooled (ZFC) and field cooled (FC) procedures were performed in a Quantum Design Magnetic Properties Measurement System (MPMS) magnetometer, in the temperature range between 5 and 300 K, applying magnetic fields up to ± 3 T. ac susceptibility measurements were also carried out applying a driving magnetic field amplitude of 2 Oe for different frequency values in the range 10–1000 Hz after the samples had been submitted to a ZFC process.

3. Results and discussion

Fig. 2 shows the temperature dependence of the ZFC (open dots) and FC (closed dots) magnetization, $M(T)$ curves, for sample *A* [panel (a)] and sample *B* [panel (b)] obtained under an applied magnetic field of 50 Oe. Each ZFC curve describes a wide peak centered at $T_B \simeq 135$ K for sample *A* and $T_B \simeq 185$ K for sample *B*,

* Corresponding author at: Grup de Magnetisme, Dept. Física Fonamental, Facultat de Física, Universitat de Barcelona, Martí i Franquès 1, planta 4, edifici nou, 08028 Barcelona, Spain.
E-mail address: agarciasan@ub.edu (A. García-Santiago).

http://dx.doi.org/10.1016/j.jmmm.2014.02.080
0304-8853

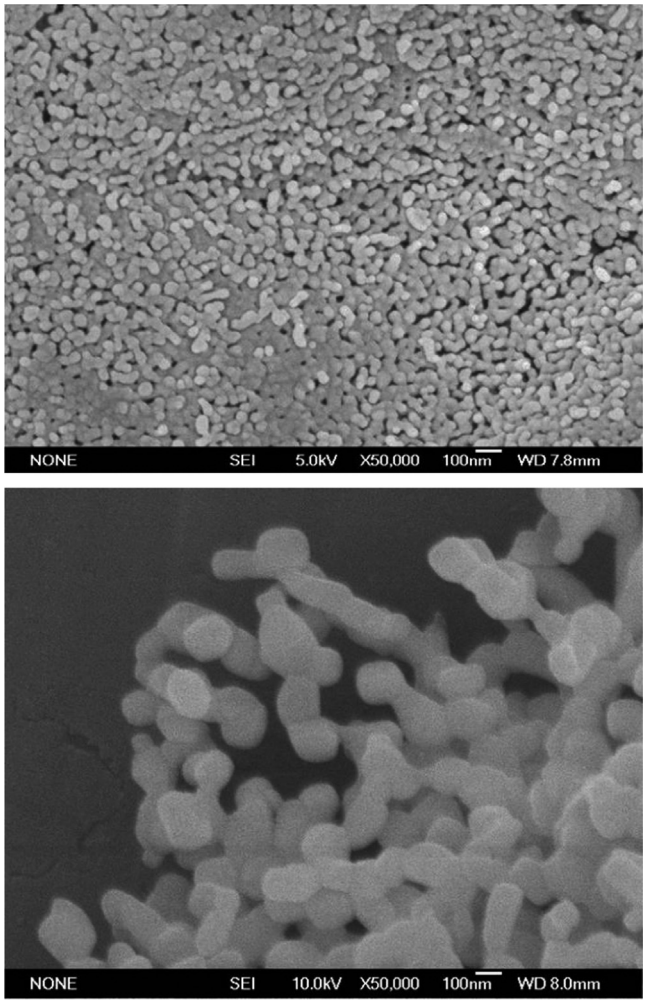

Fig. 1. Scanning electron microscope (SEM) images obtained for sample *A* (top panel) and sample *B* (bottom panel). The scale (100 nm) is shown at the bottom of the images.

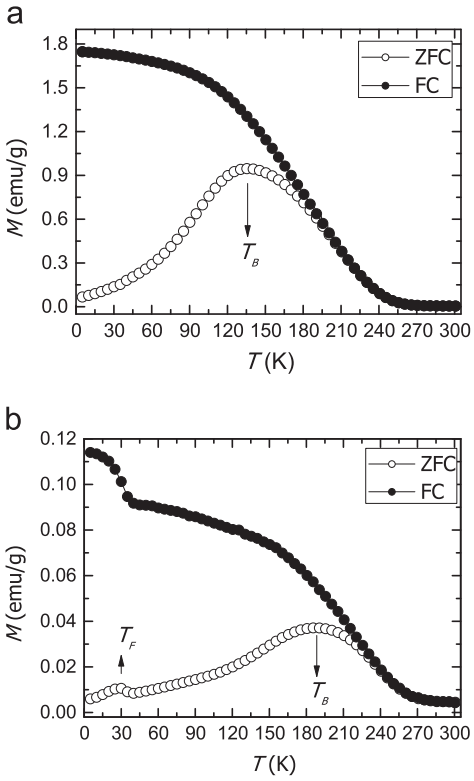

Fig. 2. Temperature dependence of the zero-field cooled (ZFC, open dots) and field cooled (FC, closed dots) magnetization obtained for sample *A* (a) and sample *B* (b) in a magnetic field of 50 Oe.

which is commonly interpreted as the signature of a magnetic blocking transition of the FM clusters with a broad distribution of sizes [4], indicating the presence of such clusters in our samples. In addition, a smaller peak centered at $T_F \simeq 30$ K is displayed in the ZFC curve in panel (b), suggesting a second transition involving the formation of another sort of FM clusters, as supported by the fast increase of the magnetization around the same temperature in the FC curve. The fact that the magnetization values are around ten times larger for sample *A* than for sample *B* can be ascribed to a higher FM-surface/AFM-core ratio in the former.

Fig. 3 presents FC magnetization measurements performed under an applied magnetic field of 2 T in the same range of temperatures as in Fig. 2. The curve shown in panel (b) for sample *B* reveals a high-temperature peak around 260 K which is similar to the one observed for the AFM/CO transition in bulk samples of this manganite [15]. Moreover, following the procedure described in Ref. [15], a value of $T_{CO} \simeq 235$ K has been determined from the derivative of this curve, which agrees with bulk values commonly reported in the literature [2,4,15]. This peak is completely absent for sample *A* in panel (a), where the curve resembles the FC one plotted in Fig. 2(a) for $H = 50$ Oe. This indicates that the size effects in sample *B* are not strong enough to hide AFM bulk properties at 2 T, while the grains in sample *A* manifest only FM properties at these experimental conditions, in accordance with the behavior discussed in Fig. 2.

Panels (a) and (b) in Fig. 4 show the temperature dependence of the real part of the ac susceptibility, χ', for sample *A* and sample *B*, respectively (see the legend for frequency values). Both curves display broad peaks, similar to those observed in the ZFC dc magnetization curves in Fig. 2, but they are centered at temperature values (around 155 K for sample *A* and 205 K for sample *B*) which are slightly larger than their respective T_B values (around 135 K for sample *A* and 185 K for sample *B*), as expected for a blocking temperature. However, as the frequency increases, although the χ' value at the peak tends to shrink for both samples, the centering temperature values do not change, which is not the behavior expected for superparamagnetic (SPM) clusters, SGs or CGs [14]. The appearance of the peak in our samples should be then mostly related to the temperature range at which the anisotropy energy barriers begin to vanish due to the loss of magnetic ordering as the temperature increases, and this would explain why the position of such peak does not depend on frequency. The temperature of magnetic ordering, T_{MO}, can be defined at the inflection point of the χ' curves to be around 235 K for sample *A* and 260 K for sample *B*. Such point matches the temperature at which all the curves superimpose, as expected for a paramagnetic state. If we focus on sample *B*, we realize a reasonable coincidence of T_{MO} with the peak position of Fig. 3(b), suggesting that all kinds of magnetic ordering transitions (FM and AFM) manifest together at the same temperature.

To complete the discussion of Fig. 4, we would like to remark the occurrence in panel (b) of a frequency-independent tiny peak which coincides with the position of T_F found in Fig. 2(b) around 30 K for sample *B*. In order to shed light on the transition associated to this peak, a genuine ZFC protocol was followed on this sample. This kind of memory effect measurement consists in a ZFC process from 300 K to a certain temperature below T_F, that in this case was chosen as 12 K, at which the sample was then aged for a waiting time of 3 h. Afterwards the system was further cooled

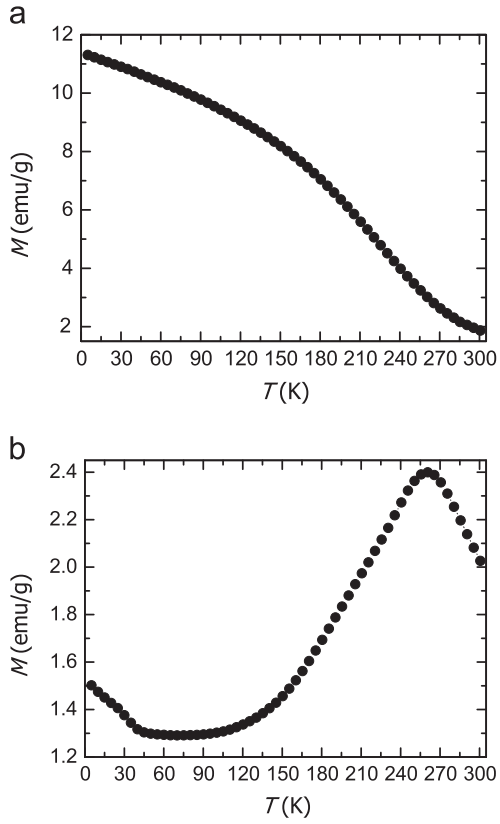

Fig. 3. Temperature dependence of the field cooled (FC) magnetization obtained for sample *A* (a) and sample *B* (b) in a magnetic field of 2 T.

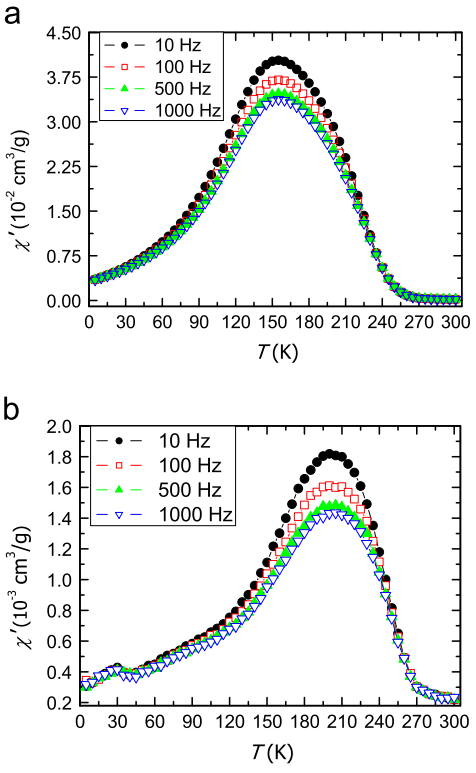

Fig. 4. Temperature dependence of the real part of the ac magnetic susceptibility for sample *A* (a) and sample *B* (b) obtained by applying an ac magnetic field of 2 Oe for different frequency values (see the legend for details) after each sample had been submitted to a ZFC process.

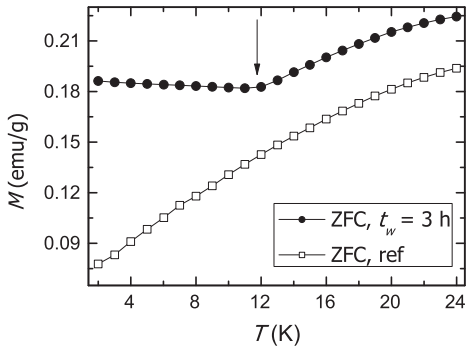

Fig. 5. Genuine (solid dots) and standard (open squares) ZFC magnetization curves obtained for sample *B* under an applied magnetic field of 750 Oe.

down to 2 K and the magnetization was subsequently measured under an applied magnetic field of 750 Oe between 2 K and 24 K. The result of this process is plotted (solid dots) in Fig. 5 together with the curve (open squares) obtained when a standard ZFC protocol was followed in the same range of temperature under the same applied magnetic field. The genuine ZFC magnetization curve displays a minimum at 12 K, indicating the memory effect of this sample, a usual feature of SG systems when the chosen aging temperature is far below their freezing temperature. We therefore suggest that $T_F \simeq 30$ K should be considered more precisely as a second magnetic transition leading to the development of SG behavior at low temperatures in sample *B* [16].

Fig. 6 shows magnetic hysteresis cycles for sample *A* [panels (a) and (d)] and sample *B* [panels (b) and (e)] obtained at 5 K following ZFC and FC protocols, the latter under an applied magnetic field of 3 T. A lateral displacement of the FC loop with respect to the ZFC one is displayed in panels (d) and (e) indicating the occurrence of EB interaction and hence confirming the presence of FM and AFM phases in both samples. The values of the EB field ($H_{EB} \simeq 420$ Oe for sample *A* and $H_{EB} \simeq 380$ Oe for sample *B*) are reasonably similar to those reported in previous works [14]. Moreover, although the lateral displacement is larger for sample *A*, the FC curve shows an overall vertical shift with respect to the ZFC one which is larger for sample *B* [see panels (a) and (b)]. This shift is almost absent at higher temperatures, as it can be observed in panels (c) and (f) in Fig. 6, where the magnetic hysteresis cycles obtained for sample *B* at 50 K following the same ZFC and FC protocols are plotted. We suggest that this effect, together with the results obtained in Figs. 2(b and 5, are explained considering that at low temperature the spins in the interface between the FM surface and the AFM core in every grain of sample *B* would freeze in a SG configuration. As a consequence, depending on the cooling protocol, the final frozen state may be oriented (FC process) or not (ZFC process), and this originates the vertical shift observed in the magnetic cycles at 5 K. Although the EB effect in a system including a SG component has been studied [17–19], the effect investigated here for this kind of manganites has been hardly reported [20].

4. Conclusions

In conclusion, the magnetic behavior of two nanogranular $La_{0.25}Ca_{0.75}MnO_3$ manganite samples with different average grain sizes has been experimentally investigated and has been found to be well-described by applying a core–shell model to each grain, considering an antiferromagnetic core and a ferromagnetic outer surface. Both samples show the occurrence of exchange bias effect in their magnetic hysteresis cycles, associated with the interaction

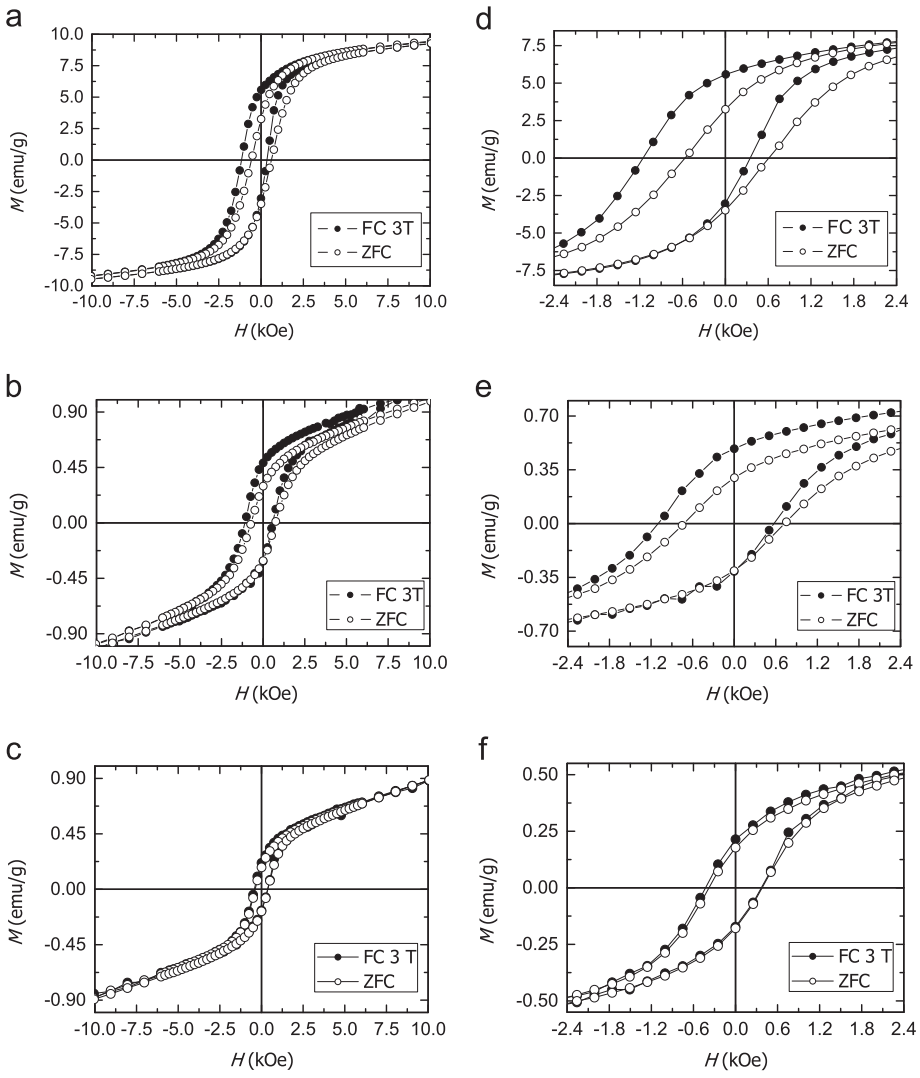

Fig. 6. Magnetic hysteresis cycles in the magnetic field range between −10 kOe and 10 kOe obtained for sample *A* at 5 K [panel (a)], and sample *B* at 5 K [panel (b)] and 50 K [panel (c)], after the samples had been cooled following ZFC (open dots) and FC-under-3-T (solid dots) protocols. Panels (d), (e) and (f) show magnifications of these cycles in the magnetic field range between −2.4 kOe and 2.4 kOe for panels (a), (b) and (c), respectively.

between these two phases. For each sample, the results suggest that magnetic ordering of both phases occurs at the same temperature. Moreover, the sample with the largest grains presents a second transition at low temperature which, together with the observation of ageing phenomena, has been interpreted as a spin-glass freezing of the spins at the interface between the ferromagnetic surface and the antiferromagnetic core of the grains. This effect is not observed in the other sample because, due to the small size of the grains, the fraction of ferromagnetic phase is dominant. Finally, it is worth being emphasized that most of these features have nothing to do with those commonly shown by nanoparticle manganites, where only spin glass or cluster glass behavior and exchange bias effect are observed in magnetic measurements.

Acknowledgments

J. M. H. acknowledges support from Spanish Ministerio de Educación y Ciencia and Universitat de Barcelona. A.G.-S. acknowledges support from Universitat de Barcelona. This work was financially supported by the Spanish Government Projects no. MAT2008-04535 and MAT2011-23698.

References

[1] E. Dagotto, T. Hotta, A. Moreo, Phys. Rep. 344 (2001) 1.
[2] A.P. Ramírez, S.-W. Cheong, P. Schiffer, J. Appl. Phys. 81 (1997) 5337.
[3] A. Biswas, I. Das, Phys. Rev. B 74 (2006) 172405.
[4] T. Zhang, T.F. Zhou, T. Qian, X.G. Li, Phys. Rev. B 76 (2007) 174415.
[5] E. Rozenberg, M. Auslender, A.I. Shames, D. Mogilyansky, I. Felner, E. Sominskii, A. Gedanken, Ya.M. Mukovskii, Phys. Rev. B 78 (2008) 052405.
[6] C.L. Lu, S. Dong, K.F. Wang, F. Gao, P.L. Li, L.Y. Lv, J.-M. Liu, Appl. Phys. Lett. 91 (2007) 032502.
[7] T. Qian, G. Li, T. Zhang, T.F. Zhou, X.Q. Xiang, X.W. Kang, X.G. Li, Appl. Phys. Lett. 90 (2007) 012503.
[8] R.S. Freitas, L. Ghivelder, F. Damay, F. Dias, L.F. Cohen, Phys. Rev. B 64 (2001) 144404.
[9] V. Markovich, I. Fita, A. Wisniewski, D. Mogilyansky, R. Puzniak, L. Titelman, C. Martin, G. Gorodetsky, Phys. Rev. B 81 (2010) 094428.
[10] T. Zhu, B.G. Shen, J.R. Sun, H.W. Zhao, W.S. Zhan, Appl. Phys. Lett. 78 (2001) 3863.
[11] L. Ghivelder, F. Parisi, Phys. Rev. B 71 (2005) 184425.
[12] T. Zhang, M. Dressel, Phys. Rev. B 80 (2009) 014435.
[13] V. Markovich, I. Fita, A. Wisniewski, R. Puzniak, D. Mogilyansky, L. Titelman, L. Vradman, M. Herskowitz, G. Gorodetsky, Phys. Rev. B 77 (2008) 054410.

[14] X.H. Huang, J.F. Ding, G.Q. Zhang, Y. Hou, Y.P. Yao, X.G. Li, Phys. Rev. B 78 (2008) 224408.
[15] M. Pissas, I. Margiolaki, K. Prassides, E. Suard, Phys. Rev. B 72 (2005) 064426.
[16] S.P. Pati, S. Kumar, D. Das, Mater. Chem. Phys. 137 (2012) 303.
[17] M. Ali, P. Adie, C.H. Marrows, D. Greig, B.J. Hickey, R.L. Stamps, Nat. Mater. 6 (2007) 70.
[18] F.-T. Yuan, J.-K. Lin, Y.D. Yao, S.-F. Lee, Appl. Phys. Lett. 96 (2010) 162502.
[19] C. Cirillo, A. García-Santiago, J.M. Hernandez, C. Attanasio, J. Tejada, J. Phys.: Condens. Matter 25 (2013) 176001.
[20] V. Markovich, R. Puzniak, D. Mogilyansky, X. Wu, K. Suzuki, I. Fita, A. Wisniewski, S. Chen, G. Gorodetsky, J. Phys. Chem. C 115 (2011) 1582.